ORIGINAL ARTICLE

Defective lysosomal storage in Fabry disease modifies mitochondrial structure, metabolism and turnover in renal epithelial cells

Anke Schumann[1] | Kristin Schaller[1] | Véronique Belche[1] |

Markus Cybulla[2] | Sarah C. Grünert[1] | Nicolai Moers[3] | Jörn O. Sass[3] |

Andres Kaech[4] | Luciana Hannibal[5] | Ute Spiekerkoetter[1]

[1]Department of General Paediatrics, Adolescent Medicine and Neonatology, Medical Center-University of Freiburg, Faculty of Medicine, Freiburg, Germany

[2]Center of Internal Medicine, Department of Nephrology and Rheumatology, Fachinternistische Gemeinschaftspraxis Markgraeflerland, Muellheim, Germany

[3]Department of Natural Sciences, Institute for Functional Gene Analytics (IFGA), Bonn-Rhein-Sieg University of Applied Sciences, Rheinbach, Germany

[4]Center for Microscopy and Image Analysis, University of Zurich, Zurich, Switzerland

[5]Department of General Paediatrics, Adolescent Medicine and Neonatology, Laboratory of Clinical Biochemistry and Metabolism, Medical Center-University of Freiburg, Faculty of Medicine, Freiburg, Germany

Correspondence
Anke Schumann, Department of General Paediatrics, Adolescent Medicine and Neonatology Medical Center, University of Freiburg Mathildenstr. 1, 79106 Freiburg, Germany.
Email: anke.schumann@uniuklinik-freiburg.de

Abstract

Fabry disease (FD) is an X-linked lysosomal storage disorder. Deficiency of the lysosomal enzyme alpha-galactosidase (GLA) leads to accumulation of potentially toxic globotriaosylceramide (Gb3) on a multisystem level. Cardiac and cerebrovascular abnormalities as well as progressive renal failure are severe, life-threatening long-term complications. The complete pathophysiology of chronic kidney disease (CKD) in FD and the role of tubular involvement for its progression are unclear. We established human renal tubular epithelial cell lines from the urine of male FD patients and male controls. The renal tubular system is rich in mitochondria and involved in transport processes at high-energy costs. Our studies revealed fragmented mitochondria with disrupted cristae structure in FD patient cells. Oxidative stress levels were elevated and oxidative phosphorylation was upregulated in FD pointing at enhanced energetic needs. Mitochondrial homeostasis and energy metabolism revealed major changes as evidenced by differences in mitochondrial number, energy production and fuel consumption. The changes were accompanied by activation of the autophagy machinery in FD. Sirtuin1, an important sensor of (renal) metabolic stress and modifier of different defense pathways, was highly expressed in FD. Our data show that lysosomal FD impairs mitochondrial function and results in severe disturbance of mitochondrial energy metabolism in renal cells. This insight on a tissue-specific level points to new therapeutic targets which might enhance treatment efficacy.

1 | INTRODUCTION

Fabry disease (FD, OMIM #301500) is an X-linked lysosomal storage disorder caused by mutations of the enzyme alpha-galactosidase A (GLA). GLA deficiency leads to systemic accumulation of globotriaosylceramide (Gb3) and related glycosphingolipids in the lysosomes of multiple tissues.[1] Life-threatening end-organ damage like chronic kidney disease (CKD) and cardio-/cerebrovascular disease are the major clinical manifestations. Remarkably, many heterozygous females are symptomatic.[2]

Enzyme replacement therapy (ERT) reduces Gb3 concentrations and can prevent tissue-remodeling and organ damage for example, in target tissues like heart and kidney.[3-5] Treatment success depends largely on its early initiation.[6] However, therapy fails to sufficiently halt disease progression in different tissues, particularly in the kidney.[7,8] This led to the hypothesis that apart from storage of toxic metabolites, biochemical alterations promote tissue dysfunction by interference with intracellular organelles (eg, mitochondria) and activation of inflammatory pathways: Gb3 accumulation has been related to increased reactive oxygen species (ROS) in endothelial cells inducing mitochondrial dysfunction while impaired mitochondria are a source of ROS themselves.[9] Fibroblast studies linked mitochondrial dysfunction to reduced activities of respiratory chain complexes and an intracellular reduction of energy-rich phosphates underlining the impact of lysosomal FD on mitochondrial energy metabolism.[10] The release of pro-inflammatory cytokines[11] might be another disease-promoting factor since fibrotic changes have been identified as early signs of cardiac involvement.[12]

These important findings described hold also true for the kidney where storage of Gb3 was associated with an increased ROS production in podocytes[3] and dysregulated autophagy has been associated with podocyte damage.[3,13] Recent data indicate that FD not only affects glomerular but also extends to renal tubular cells[14,15] as evidenced by a loss of tubular proteins and tubular interstitial fibrosis occurring early in FD.[16]

But how to connect mitochondria-rich renal tubular cells performing transport processes at high energy costs to a lysosmal disease? Studies suggest a constant functional cross talk-between these organelles to maintain metabolic homeostasis.[17,18] Disruption of mitochondrial homeostasis drives kidney tubule dysfunction[19] whereas

Synopsis

Disruption of mitochondrial homeostasis and energy metabolism drives renal disease in a human model for Fabry disease.

its pharmacological recovery is protective.[20] Thus, dysfunctional parts of the mitochondrial network are selectively eliminated by organelle-specific mitophagy or general autophagy.[21] This quality control process is supported by NAD-dependent deacylases (sirtuins), which are crucial for metabolic adaptive stress responses.[22] Particularly sirtuin 1 (SIRT1) is an important (renal) gatekeeper controlling pathways which counteract oxidative stress, inflammation and fibrosis and promote mitochondrial biogenesis.[23]

We hypothesized that FD is a relevant stress factor for tubular cells and impacts on intracellular energy metabolism. In this study, we characterized a human renal epithelial cellular model with organ-specific features of FD. The study identified altered mitochondrial morphology and function in FD as potential drivers of CKD and reports on major differences in mitochondrial energy production and the use of cellular fuels. Autophagic activity was increased in FD patient cells. The observed shifts in mitochondrial energy metabolism were counteracted by activation of mitochondrial biogenesis and the sirtuin system.

2 | MATERIALS AND METHODS

2.1 | Cell culture

Human renal tubular epithelial cells were obtained from urine of age- and gender-matched healthy donors (n = 3) or genetically confirmed male patients (n = 3) with FD as previously described.[24-26] Patient cells were collected prior to ERT (agalsidase-alpha 0.2 mg/kg/14 days). After 2 cycles of primary culture to expand cell numbers, cells were immortalized using a pRNS1 vector.[24] The cells were cultured in DMEM Glutamax (Thermo Fisher Scientific) supplemented with 24.75 mM glucose, 10% fetal calf serum (FBS), with antibiotics streptomycin (100 μg/mL) and penicillin (100 I.U./mL). For Seahorse analysis of

oxygen consumption rate (OCR) and extracellular acidification rate (ECAR) a modified DMEM medium pH 7.4 medium was used (without phenol red, bicarbonate or FBS, supplemented with 10 mM glucose, 2 mM glutamine and 1 mM pyruvate).

2.2 | Cell viability assay

Cell viability was determined by the Cell Counting Kit-8 assay (Dojindo) according to the manufacturer's protocol. Cells were seeded at a density of 5000 cells/well and measured at 450 nm in a TECAN infinite 200 reader (Männedorf, Switzerland).

2.3 | Determination of Gb3 in cells

The concentration of Gb3 was determined by LC-MS/MS according to a published procedure with modifications.[27]

2.4 | Immuno-fluorescent staining

The cells were fixed with 4% paraformaldehyde in PBS, quenched with 50 mM NH_4Cl and permeabilized for 30 minutes in blocking buffer solution containing 0.1% Triton X-100 and 0.5% BSA dissolved in PBS. The cells were incubated overnight with the primary antibodies at 4°C. After washing with PBS, the slides were incubated for 30 minutes with fluorophore-conjugated Alexa secondary antibodies (Invitrogen, Thermo Fisher Scientific), mounted with the Prolong Gold Anti-fade reagent, and analyzed by using a Leica SP8 confocal laser scanning microscope.

2.5 | Confocal microscopy

Fluorescence images were recorded on an inverted confocal microscope (TCS SP8 X, Leica Microsystems) using a 63x oil immersion objective. 405 nm and 670 nm laser light were used for imaging the (DAPI/Hoechst) and the AlexaFluor-680 (Alexa Fluor, Invitrogen, Thermo Fischer Scientific) fluorescence, respectively.

2.6 | Electron microscopy

Cells were grown in their standard cell culture medium on 12 mm cover glasses coated with L-polylysine. Cells were sequentially fixed with 2.5% glutaraldehyde in 0.1 M sodium cacodylate buffer (pH 7.35, pre-warmed to 37°C) for 1 hour, with 1% osmium tetroxide for 1 hour in 0.1 M cacodylate buffer at 0°C, and 2% aqueous uranyl acetate for 1 hour at 4°C. Samples then were dehydrated in an ethanol series and embedded in Epon/Araldite (Sigma-Aldrich). Ultrathin (70 nm) sections were post-stained with lead citrate and examined with a Talos 120 transmission electron microscope at an acceleration voltage of 120 KV using a Ceta digital camera and the MAPS software package (Thermo Fisher Scientific).

2.7 | Extracellular flux analysis and metabolic assays

OCR and ECAR were measured in a Seahorse XFp Analyzer (Agilent) as described in the user guide for the "Agilent Seahorse XFp Real-Time ATP Rate Assay," first edition of Oct. 2018: https://www.agilent.com/cs/library/usermanuals/public/103591-400_Seahorse_XFp_ATP_Rate_Assay_Kit_User_Guide.pdf. OCR and ECAR data were converted into ATP production rates using the Agilent Seahorse XF Real-Time ATP Rate Assay Report Generator, a Microsoft Excel Macro. Culture medium conditions are provided in supporting information. Normalization was done based on protein determination according to Lowry et al. 1951.[28]

2.8 | Targeted analysis of metabolites

Polar and non-polar metabolites were determined by LC-MS/MS as previously published[29] as well as standardized procedures available in the laboratory. For details, please see supporting information.

2.9 | Immuno-blotting

Immuno-blotting was used to detect the following proteins: AQP1/2, LCN2, PINK1, SQSTM1, PGC-1 α, SIRT1, TOMM20. Proteins were lysed followed by sonication. The samples were normalized for protein (40 μg/lane), dissolved in Laemmli sample buffer and separated by SDS-PAGE in reducing conditions. After blotting onto a nitrocellulose membrane and blocking with 5% non-fat milk (1706404, Bio-Rad Laboratories), the membranes were incubated overnight at 4°C with primary antibody, washed, incubated with peroxidase-labeled secondary antibody, and visualized with chemiluminescence (WBKLS0050, Millipore, Life technologies). Quantitative analysis was performed by measuring the relative density of each band normalized to γ-tubulin using ImageJ software (imagej.nih.gov).

2.10 | Statistical analysis

The quantitative data were expressed as mean $\pm$ SD. Differences between experimental groups were evaluated using paired two tailed Student's t-tests. The sample size of each experimental group is described in the figure legends. The results are representative of at least three independent experiments. GraphPad Prism software was used for all statistical analyses. Statistical significance was set at $P \leq .05$.

3 | RESULTS

3.1 | Characterization of human renal tubular epithelial cell lines

Human renal tubular epithelial cell lines of healthy male controls (Control, n = 3) and male FD patients (FD, n = 3) were generated as previously described.[24] All FD patients suffer from severe and early onset kidney involvement (Table 1) with rapid progression to CKD. Immuno-blotting for the kidney segment specific marker proteins aquaporin 1 (AQP1) and aquaporin 2 (AQP2) (Figure 1A) confirmed a mixed culture of proximal and distal tubular epithelial renal cells. LC-MS/MS studies revealed significantly elevated levels of creatinine in FD patient cells pointing at impaired kidney function (Figure 1B). Elevated levels of lipocalin 2 (LCN2), a marker protein for kidney damage, support renal damage in FD patients (Figure 1C). Gb3 is expressed in high amounts in FD patient lysates (Figure 1D) and their cellular viability is markedly reduced (Figure 1E).

3.2 | Mitochondrial morphology and function are altered in FD

The kidney is one of the most energy-demanding organs in the human body. We therefore investigated mitochondrial morphology using immuno-fluorescent staining for TOMM20, an outer mitochondrial membrane protein. While control cells showed filamentous and extended mitochondrial networks, FD patients depicted short-statured mitochondria with predominantly perinuclear clustering (Figure 2A).

Electron microscopy (EM) revealed ultrastructural changes in FD showing swollen mitochondria and disorganized cristae structure (Figure 2A) suggesting mitochondrial involvement of renal tubular cells in lysosomal FD.

3.3 | Altered redox metabolism and mitochondrial respiration in FD

Abnormalities in mitochondrial morphology and organization of the mitochondrial network prompted us to examine mitochondrial function.

The glutathione system is one of the most efficient protectors against different ROS.

Patient cells showed 2.2-fold elevated concentrations of oxidized glutathione (GSSG) as compared to controls (Figure 2B). The ratio of reduced glutathione (GSH) to GSSG was significantly reduced underlining the presence of ROS and the need for protection in FD (Figure 2B). These data were supported by higher levels (2.3-fold) of oxidized cystine (CSSC) in FD patient cells and a decreased ratio of reduced cysteine (Cys) to CSSC (Figure 2B).

TABLE 1 Clinical information on male patients with FD

	Control 1	Control 2	Control 3	FD 1	FD 2	FD 3
Mutation				c.718_719delAA	c.1031T>C	c.959A>T
Exon				5	7	6
Age at CKD onset				20	16	24
Creatinine (mg/dl)	0.6	0.5	0.6	1.6	1.3	2.8
eGFR (ml/min/1.73 m^2)	112	115	110	49	63	24
CKD stage				GIIIa	GII	GIV
Heart involvement				Yes	Yes	Yes
Stroke				No	Yes	No
Hearing impairment				No	Yes	Yes
Cornea verticillata				Yes	Yes	Yes
MSSI				32	51	63

Note: All patients received enzyme replacement therapy. The patients are suffering from CKD stage GII-GIV as defined by Levy. Formula used for eGFR-calculation; CKD-EPI. The patients suffer from multi-organ involvement. Mainz severity score index (MSSI): mild: <20, moderate 20-40, severe >40.[30]
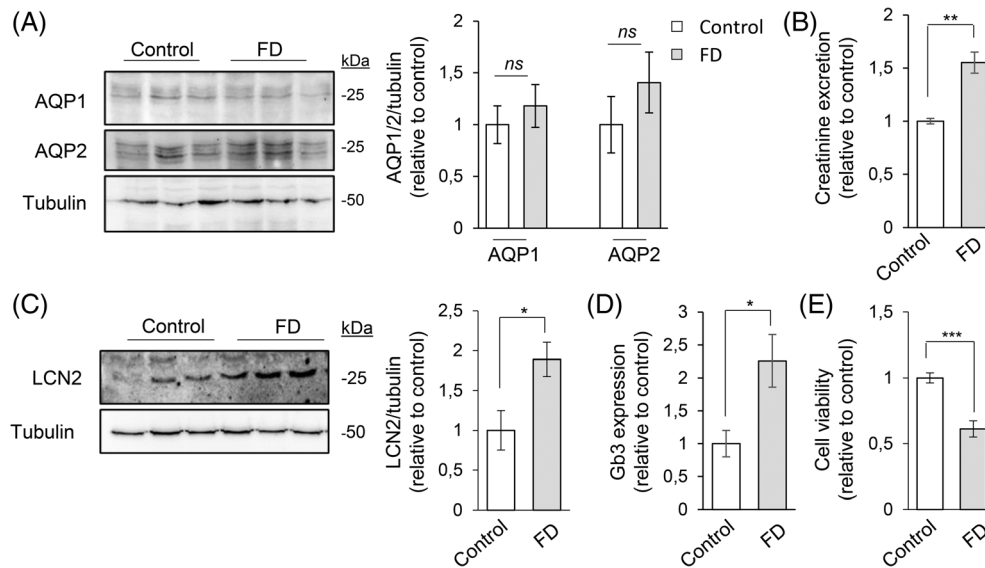
FIGURE 1 Characterization of human renal tubular epithelial cell lines. A, Immuno-blot analysis and quantification for aquaporin (AQP) 1 and AQP2 in control and Patient cells (FD). Tubulin was used as loading control; *ns*: not significant. B, LC-MS/MS quantification of creatinine; n = 12 per group. **$P \leq .004$. C, Immuno-blot analysis and quantification for lipocalin 2 (LCN2) in control and patient cells (FD). Tubulin was used as loading control. *$P \leq .04$. D, LC-MS/MS quantification of globotriaosylceramide (Gb3) in cell lysates; n = 9 per group. *$P \leq .03$. E, Cell viability assay in control and patient (FD) cells; n = 12 per group. ***$P \leq .0002$
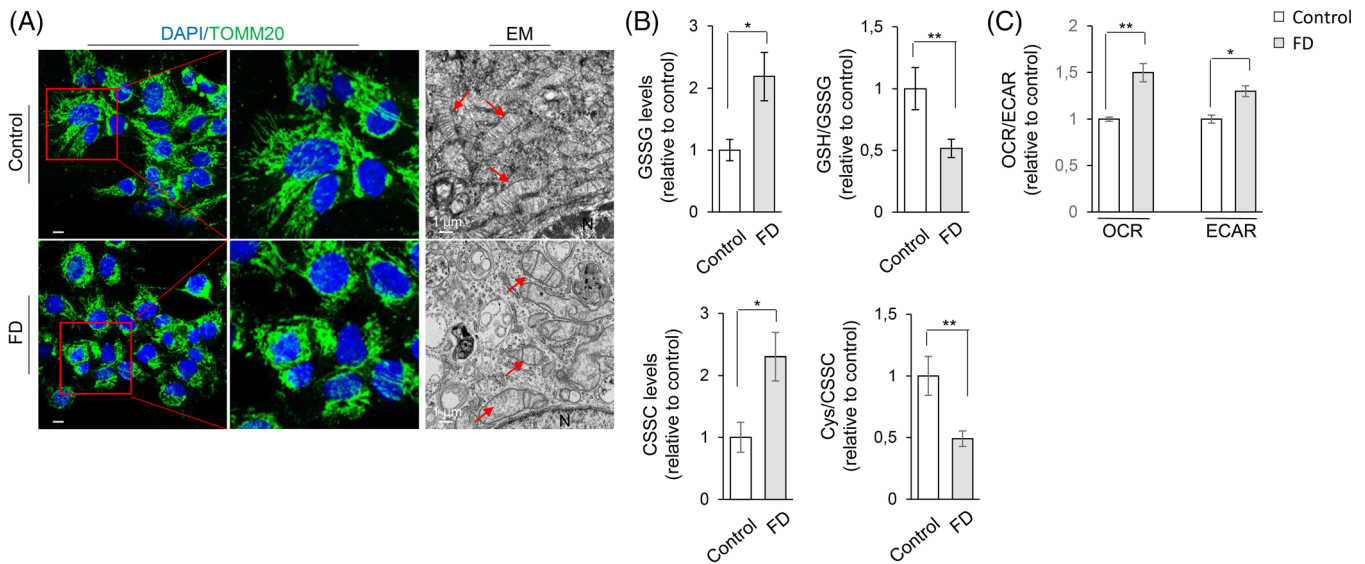
FIGURE 2 Changes in mitochondrial morphology and function. A, Cells were immuno-stained with translocase of the outer mitochondrial membrane 20 (TOMM20) antibody (green) and analyzed by confocal microscopy. Nuclei counter stained with 4′,6-diamidino-2-phenylindole (DAPI, blue). Red squares contain images at higher magnification. Scale bar: 10 μm. Electron microscopy showing representative micrographs of mitochondria (red arrows) in control and FD patient cells. N = nucleus. Scale bar: 1 μm. B, Upper panel: Quantitative LC-MS/MS analysis of oxidized glutathione (GSSG) and ratio of GSSG to reduced glutathione (GSH). *$P \leq .04$; **$P \leq .01$. Lower panel: Quantitative LC-MS/MS analysis of oxidized cystine (CSSC) and ratio of CSSC to reduced levels of cysteine (Cys). *$P \leq .03$; **$P \leq .009$; n = 12 per group. C, Seahorse analysis of control and FD patient cells. Oxygen consumption rate (OCR) and extracellular acidification rate (ECAR) are expressed relative to control. n = 12 measurements per cell line; *$P \leq .028$; **$P \leq .014$

Seahorse data analysis (Figure 2C) revealed that FD cells have a greater OCR and increased ECAR (Figure 2C) compared to control cells. The Seahorse experiment was conducted under assay conditions including a block in oxidative phosphorylation. The modified DMEM medium utilized for OCR and ECAR

measurements is depleted of FCS and supplemented with pyruvate.

3.4 | Tricarboxylic citric acid cycle remodeling in FD

By linking major catabolic pathways with mitochondrial energy production, intermediary metabolites of the tricarboxylic citric acid (TCA) cycle are involved in maintaining intracellular and tissue homeostasis and play a crucial role in intracellular signaling.

We performed LC-MS/MS analyses of cell lysates and cell culture medium. FD patients' lysates show high concentrations of the important TCA cycle intermediates alpha-ketoglutarate (7.9-fold elevated), succinate (2.8-fold elevated) and citrate (1.9-fold elevated), suggesting an accumulation of these metabolites. Methylcitrate was slightly elevated (1.3-fold) in FD patient cells (Figure 3A). In contrast, intracellular lactate and malate levels were decreased to 60% of control levels (Figure 3A).

The concentration of itaconate was markedly elevated (1.9-fold) in the cell culture medium of FD patient cells indicating secretion of this metabolite (Figure 3B). Alpha-ketoglutarate (43% of control) and methylcitrate (54% of control) concentrations were significantly reduced (Figure 3B), reflecting the intracellular conditions where the precursors are retained for energy production.

3.5 | Substrate utilization in FD: fatty acid and amino acid metabolism

Because we noted abnormal oxidative phosphorylation in FD cells, we examined the status of turnover of fatty acids, a fuel for energy production in renal cells.[31-35]

The levels of free carnitine and short-chain acylcarnitines are comparably high in FD cells. However, FD cells show significantly lower levels of medium- (16% of control) and long-chain acylcarnitines (7% of control) pointing at activated utilization of fatty acids for beta-oxidation (Figure 4A). This up-regulation in the use of medium- and long-chain acylcarnitines may represent a mechanism to support energy production under conditions where oxidative phosphorylation is compromised in FD cells (see above).

Amino acids were equally distributed in both cellular lysates and medium in FD and control cells (Figure 4B). The only exception was glutamine, which was 2.2-fold elevated in FD patients cell lysates (Figure 4B). Interestingly, glutamine is converted into alpha-ketoglutarate, a
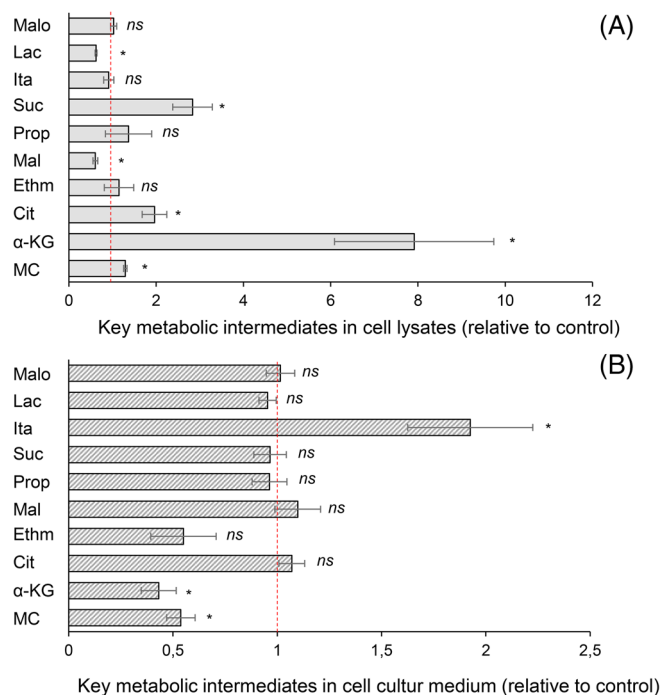
FIGURE 3 Tricarboxylic citric acid cycle remodeling in FD. A, Quantitative LC-MS/MS analysis of tricarboxylic citric acid cycle metabolites in cell lysates. Data are expressed relative to control (dotted red line); n = 6 per group. MC: methylcitrate (*$P \leq .02$), α-KG: alpha-ketoglutarate (*$P \leq .03$), Cit: citrate (*$P \leq .03$), Ethm: ethylmalonate, Mal: malate (*$P \leq .03$), Prop: propionate, Suc: succinate (*$P \leq .05$), Ita: itaconate, Lac: lactate (*$P \leq .05$), Malo: malonate; *ns*: not significant. B, Quantitative LC-MS/MS analysis of tricarboxylic citric acid cycle metabolites in cell culture medium. Data expressed relative to control (dotted red line); n = 6 per group. MC: methylcitrate (*$P \leq .02$), α-KG: alpha-ketoglutarate (*$P \leq .019$), Cit: citrate, Ethm: ethylmalonate, Mal: malate, Prop: propionate, Suc: succinate, Ita: itaconate (*$P \leq .05$), Lac: lactate, Malo: malonate; *ns*: not significant

metabolite which is already enriched in the cellular system (Figure 3A).

3.6 | Activation of autophagy

Triggered by metabolic stress, highly energy dependent cells use organelle-specific mitophagy or autophagy to remove toxic products and dysfunctional organelles. To initiate mitophagy the protein kinase PINK1 accumulates on the outer mitochondrial membrane,[21] where it recruits other autophagic receptors.[21,23] Compared to control cells we did not observe any difference in PINK1 expression between control and patient cells (Figure 5A), revealing that the organelle-specific degradation pathway is not activated.
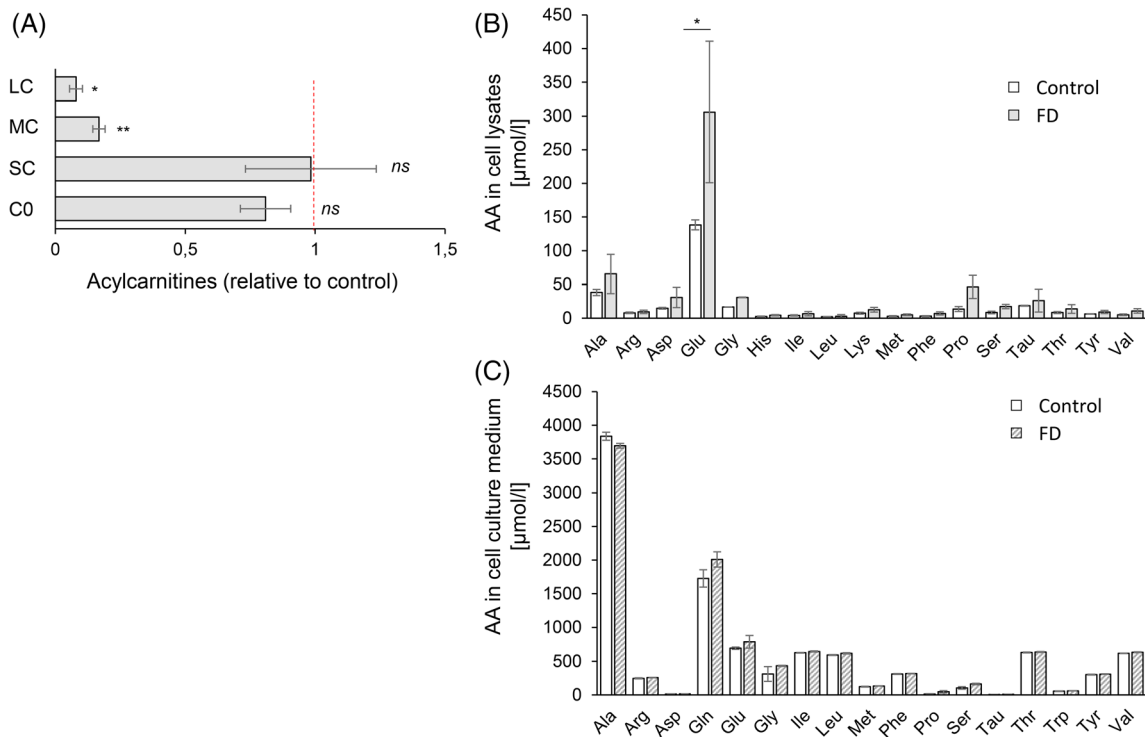
FIGURE 4 Substrate utilization in FD. A, Acylcarnitine profile performed in crude cell lysates of control and FD patient cells. Data are expressed relative to control (dotted red line). C0: free carnitine, SC: short-chain acylcarnitine, MC: medium-chain acylcarnitine (**$P \leq .003$), LC: long-chain acylcarnitine (*$P \leq .05$); n = 12 per group; *ns*: not significant. B, Amino acid (AA) profile [μmol/l] in cell lysates of control and FD patient cells. Ala: alanine, Arg: arginine, Asp: asparagine, Glu: glutamate, Gly: glycine, His: histidine, Ile: isoleucine, Leu: leucine, Lys: lysine, Met: methionine, Phe: phenylalanine, Pro: proline, Ser: serine, Tau: taurine, Thr: threonine, Tyr: tyrosine, Val: valine. n = 12 per group, ($P^* \leq .03$). White and gray bars indicate controls and FD patients, respectively. C, Amino acid (AA) profile [μmol/l] in cell culture medium of control and FD patient cells. Ala: alanine, Arg: arginine, Asp: asparagine, Glu: glutamate, Gly: glycine, His: histidine, Ile: isoleucine, Leu: leucine, Lys: lysine, Met: methionine, Phe: phenylalanine, Pro: proline, Ser: serine, Tau: taurine, Thr: threonine, Tyr: tyrosine, Val: valine. n = 12 per group. White and gray bars indicate controls and FD patients, respectively
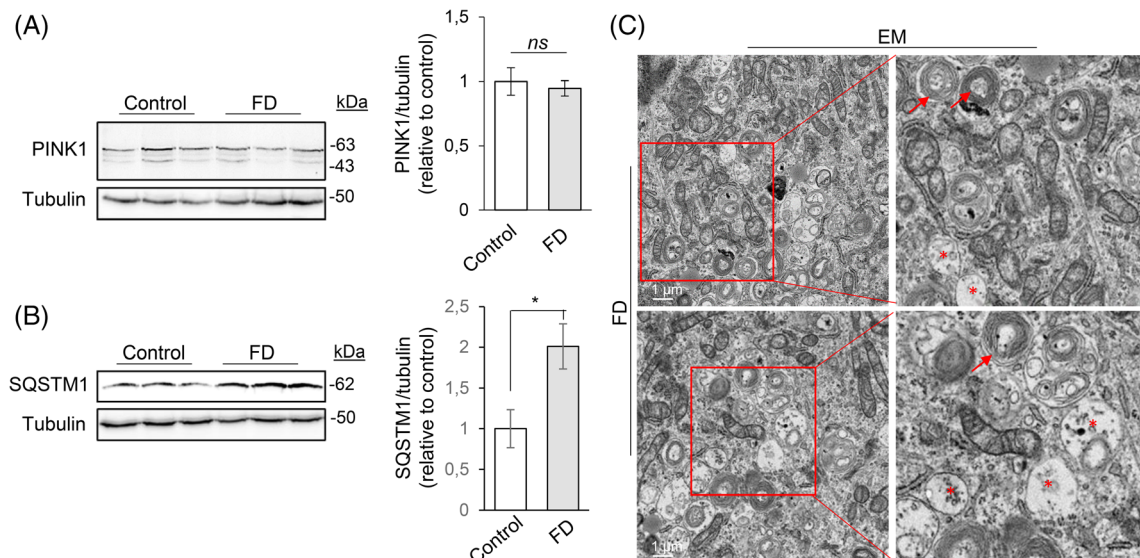
FIGURE 5 A, Immuno-blot analysis and quantification for PTEN-induced kinase 1 (PINK1) in control cells and patient cells (FD). Tubulin was used as loading control; *ns*: not significant. B, Immuno-blot analysis and quantification for Sequestosome-1 (SQSTM1) in control and patient cells (FD). Tubulin was used as loading control. (*$P \leq .03$). C, Electron micrographs showing autophagic vacuoles (red *) and FD-specific myelin-like, lamellar inclusion bodies (red arrows). Scale bar: 1 μm

SQSTM1 is an autophagy substrate and used as reporter of autophagic activity.[36] Immuno-blot analysis revealed elevated levels of SQSTM1 (1.9-fold) in FD patients pointing at a highly active autophagy machinery (Figure 5B). Activation of autophagy is an energy demanding process[36] and may serve as a mechanism to diminish the effects of toxic Gb3. EM investigations revealed vast amounts of autophagic vacuoles containing myelin-like lamellar bodies which have been associated withGb3 accumulation (Figure 5C).[37]

3.7 | Preservation of mitochondrial homeostasis in FD

Due to the identified changes we aimed to investigate the impact of FD on mitochondrial homeostasis. Immuno-blot analysis for TOMM20, a mitochondrial marker protein, revealed an increase of mitochondrial mass (2.4-fold) in FD cells (Figure 6A,D). This gain was due to activation of mitochondrial biogenesis. Peroxisome proliferator-activated receptor gamma coactivator 1-alpha (PCG1-α), the master regulator of mitochondrial biogenesis, was elevated 1.6-fold in FD patient cells (Figure 6A,B). Sirtuins are NAD-dependent deacylases
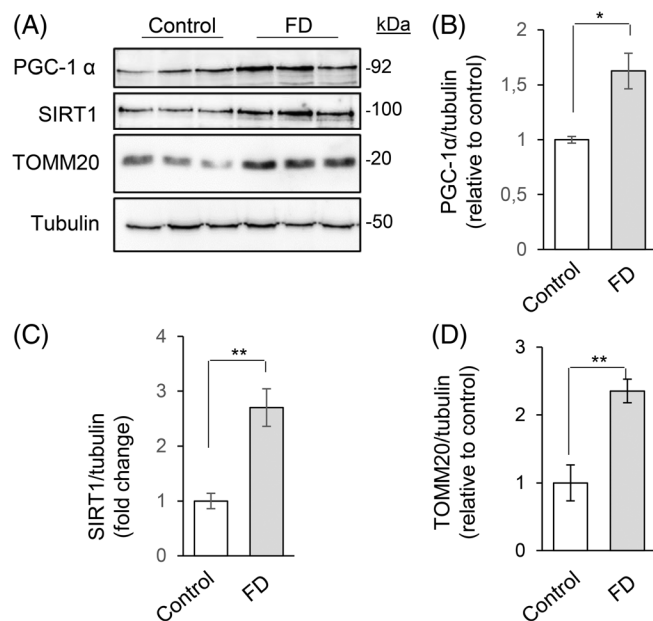

FIGURE 6 A, Immuno-blot analysis for Peroxisome proliferator-activated receptor gamma coactivator 1-alpha (PGC-1 α), Sirtuin 1 (SIRT1) and translocase of the outer mitochondrial membrane 20 (TOMM20) in control and patient cells (FD). B, Quantitative analysis for PGC-1 α. Tubulin was used as loading control. (*$P \leq .03$). C, Quantitative analysis for SIRT1. Tubulin was used as loading control. (**$P \leq .008$). D, Quantitative analysis for TOMM20. Tubulin was used as loading control. (**$P \leq .01$)

and widely expressed in the renal tubular system.[22] SIRT1 has recently been linked to adaptive stress response regulating important pathways such as anti-oxidative stress response, anti-inflammatory and anti-apoptotic pathways.[22] Immuno-blotting revealed elevated levels of SIRT1 (3.2-fold elevated) in FD patient cells as compared to controls (Figure 6A,C) indicating that this rescue system is active.

4 | DISCUSSION

In this study, we established a human renal disease model for FD to investigate the impact of a lysosomal disease on mitochondrial homeostasis in renal tubular cells. Our study revealed major metabolic alterations in tubular cells which severely impact renal energy metabolism underlining their role for CKD progression in FD. The impact on mitochondrial function indicates novel targets for interventions.

Investigation of mitochondrial morphology revealed short-statured, swollen mitochondria with a perinuclear staining pattern and disrupted cristae structure in FD patients. This is in line with Maruyama[38] et al. who describe abnormal mitochondrial morphology in renal tubular cells in a murine FD model. Investigation of the glutathione system, one of the most important anti-oxidant systems, revealed massively elevated ROS levels in FD cells. Oxidative stress caused by Gb3 storage has been associated with FD according to respective markers in human blood and urine[39] and has been confirmed in cellular models.[9]

In functional analysis by Seahorse technology with medium devoid of FCS, cells rely on glucose and pyruvate as exogenous substrates for energy production. Pyruvate has two major fates, namely, conversion to lactate (anaerobic glycolysis) or entering the TCA cycle to undergo oxidation, with the latter stimulating cellular respiration. The observed increase in OCR in FD cells compared to healthy controls appears uncoupled from energy production, as suggested by the presence of increased ROS and relatively greater expenditure of glucose and pyruvate. Increased ECAR could be attributed to increased production of CO_2 generated via the TCA cycle and the oxidative phosphorylation (OXPHOS) system.[40] Under basal experimental conditions (FCS supplied, no pyruvate added) where cells can perform full pathway turnover for energy production, we observed decreased lactate production (decreased glycolysis) and increased fatty acid oxidation (FAO) in FD compared to healthy controls, suggesting the latter as a more readily source of ATP in FD cells. Mitochondria use beta-oxidation for energy production and the activity of FAO

has been related to concentrations of acylcarnitines.[41,42] Besides preferred consumption of medium- and long-chain acylcarnitines determined in this study, other works have also shown that renal tubular cells are equipped to perform FAO under conditions of increased energy demand wherein glycolysis may be inhibited and/or as seen in cellular repair processes.[32-36] Evidence of impaired energy metabolism in FD has also been reported in fibroblasts[10] and heart.[43] Importantly, disturbed FAO has been linked to interstitial renal fibrosis in mouse and humans[32] and lipid depletion is used to induce renal fibrosis in experimental conditions.[44] The plasticity in substrate utilization observed in our study might be organ-specific and emerge from the fact that the kidney needs to perform transport processes at high energy costs while sustaining energy-demanding autophagy for Gb3 removal[36] (see below). Uncoupled oxygen consumption by dysfunctional mitochondria results in augmentation of ROS production as observed in our experimental model, thus sustaining a vicious circle of organelle damage.[9] The observed accumulation of TCA cycle metabolites (see below) in FD patient cells points towards altered mitochondrial usage of substrates. Disturbances of mitochondrial energy metabolism have been described in other energy dependent organs like the heart.[43]

The TCA cycle is a central regulatory unit in (mitochondrial) energy metabolism and part of anabolic as well as catabolic reactions. We detected high intracellular concentrations of alpha-ketoglutarate, succinate and citrate in FD patient cells. Alpha-ketoglutarate is the substrate of the alpha-ketoglutarate-dehydrogenase complex, a major modulator of respiratory chain activity and metabolic flux through the TCA cycle.[45] Succinate represents the only direct link between the TCA cycle and the respiratory chain[46] and plays a major role in the signal transduction of inflammation, hypoxia and metabolic signaling.[46,47] As discussed by Rozenfeld et al.[48] succinate elevation might be one inflammatory mechanism stimulating CKD in renal tubular cells in FD. Citrate bridges carbohydrate and fatty acid metabolism. Due to its inhibitory effects on glycolysis, elevated citrate concentrations in FD patients thus block alternative pathways for energy generation supporting a vicious circle. In fact, under basal experimental conditions, intracellular lactate concentrations in FD patient cells are markedly reduced and beta-oxidation is up-regulated. Furthermore, citrate plays a role in the mediation of inflammatory reactions via cytokine production.[49] The pro-inflammatory signals mediated by elevated succinate and citrate concentrations need to be counterbalanced: most interestingly, itaconate is an inhibitor of methylmalonyl-CoA mutase, thus antagonizing with the replenishment of succinate.[50,51] Itaconate is secreted by

FD patients' cells in high concentrations and might protect renal tissue from the invasion of pro-inflammatory immune cells to counteract fibrotic processes.

Comparison of extra- and intracellular amino acid concentrations revealed high concentrations of glutamine in FD patient cells. Glutamine is cleaved to alpha-ketoglutarate, which in turns enters the TCA cycle. High glutamine levels might reflect inhibition of this reaction due to sufficiency of alpha-ketoglutarate, as determined in our metabolomics experiment. Furthermore, activation of autophagy and increased glutamine production have been described as metabolic response to enhanced energy demands.[52] Finally, high intracellular glutamine concentrations have been associated with CKD.[53]

Elevated levels of SQSTM1 and a vast amount of autophagic vacuoles filled with Gb3 deposits[38] suggested activated autophagy in FD patient cells. This points to an increased need for waste removal which apparently comes at high energy costs. The EM data support the fact that lysosomal digestion of Gb3 is not only defective in glomeruli but also in renal tubular cells.

We next investigated the impact of FD on renal mitochondrial homeostasis. Indeed, mitochondrial mass was increased in FD patient cells. Elevated levels of PGC-1 α suggest that this increase is due to activation of mitochondrial biogenesis. SIRT1, which is particularly expressed in proximal and distal renal tubular epithelial cells and governs mitochondrial biogenesis upstream of PGC-1 α as well as important anti-inflammatory and anti-fibrotic pathways[22] was significantly up-regulated in our system. Modulation of mitochondrial mass as compensatory mechanism to cellular damage has been discussed as rescue mechanism in different tissues, particularly in the kidney.[23,54] Of note, sirtuins are targetable by small molecules, so called "sirtuin-activating compounds" like formoterol, which are able to increase SIRT1 binding affinity and thus its mediated effects.[54,55] These substances have already been investigated for their potential protective effect in kidney disease of different origin[54,55] and thus could be interesting for further studies in FD.

Having investigated these important pathways of energy homeostasis we would like to critically point out that we studied a culture of mixed human renal tubular cells, which depending of their origin might have different primary metabolic needs and preferred energy sources. However, the kidney as a whole organ is composed of these cells forming a functional unit which we feel justifies the use of our model. Investigations of a similar renal disease-model for methylmalonic aciduria[56] revealed major differences of investigated pathways supporting disease-specific mechanisms for the FD model. Our results point to mitochondrial dysfunction as the basis for adjustments in energy production by

cells, including plasticity in substrate utilization. The exact partition of substrates between different downstream energy-producing pathways (glycolysis, FAO, TCA/OXPHOS) by isotopic tracing wherein the fate of carbon units derived from for example, universally labeled glucose or pyruvate is assessed by quantitative mass spectrometry, will be addressed in a follow-up study.

In summary, we established an organ-specific cellular model to investigate the renal epithelial cell phenotype in FD. The study identified severe disturbance of mitochondrial morphology and function in a lysosomal disease, which is reflected in TCA cycle remodeling and a preference in substrate utilization in FD cells. Autophagy is activated to balance ROS induced damage driven by massive Gb3 accumulation. Important key regulators of renal energy metabolism are mobilized, leading to preservation of mitochondrial homeostasis in FD cells. Pharmacological modification of these identified regulators might offer new treatment options for CKD in FD. Free carnitine (C0), short-chain (C2-C5), medium-chain (C6-C12) and long-chain (C12-C18).

CONFLICT OF INTEREST
The authors declare no conflicts of interest.

AUTHOR CONTRIBUTIONS
Anke Schumann: involved in generation of cell lines, study design, execution of experiments, data interpretation, preparation of manuscript; Kristin Schaller: involved in execution of experiments, Véronique Belche: involved in execution of experiments; Markus Cybulla: involved in clinical assessment of included patients; Sarah C. Grünert: involved in critical clinical evaluation of the manuscript, Nicolai Moers: involved in execution of experiments; Jörn Oliver Sass: involved in evaluation of experiments, Andres Kaech: involved in execution of experiments, Luciana Hannibal: involved in metabolomic analysis and interpretation of results, preparation of manuscript, Ute Spiekerkoetter: supervised the study. All authors critically revised the manuscript before submission.

PATIENT CONSENT/ETHICS APPROVAL
Informed consent was obtained from all individuals. All procedures were in accordance with the Helsinki Declaration of 1975, as revised in 2000 (5), and the ethical regulations of the University of Freiburg. The study has been approved by the ethical commission of the University of Freiburg (ethical vote 371/17). The study is registered in the German Clinical Trial Registry, clinical trial number: DRKS00012943. Proof that informed consent was obtained is available upon request.

DOCUMENTATION OF ETHICAL APPROVAL FROM THE INSTITUTIONAL COMMITTEE FOR CARE AND USE OF LABORATORY ANIMALS (OR COMPARABLE COMMITTEE)
No animal models have been involved in the conduction of the study.

DATA AVAILABILITY STATEMENT
The datasets generated for this study are available upon reasonable request to the corresponding author.

ORCID
Anke Schumann https://orcid.org/0000-0002-7958-0188

REFERENCES
1. Germain DP. Fabry disease. *Orphanet J Rare Dis*. 2010;5:30. https://doi.org/10.1186/1750-1172-5-30.
2. Germain DP, Fouilhoux A, Decramer S, et al. Consensus recommendations for diagnosis, management and treatment of Fabry disease in paediatric patients. *Clin Genet*. 2019;96(2):107-117.
3. Chévrier M, Brakch N, Céline L, et al. Autophagosome maturation is impaired in Fabry disease. *Autophagy*. 2010;6(5):589-599. https://doi.org/10.4161/auto.6.5.11943.
4. Germain DP, Charrow J, Desnick RJ, et al. Ten-year outcome of enzyme replacement therapy with agalsidase beta in patients with Fabry disease. *J Med Genet*. 2015;52(5):353-358. https://doi.org/10.1136/jmedgenet-2014-102797.

5. Seydelmann N, Wanner C, Störk S, Ertl G, Weidemann F. Fabry disease and the heart. *Best Pract Res Clin Endocrinol Metab.* 2015;29(2):195-204. https://doi.org/10.1016/j.beem.2014.10.003.

6. Weidemann F, Niemann M, Breunig F, et al. Long-term effects of enzyme replacement therapy on Fabry cardiomyopathy: evidence for a better outcome with early treatment. *Circulation.* 2009;119(4):524-529. https://doi.org/10.1161/circulation.108.794529.

7. Schiffmann R, Hughes DA, Linthorst GE, et al. Screening, diagnosis, and management of patients with Fabry disease: conclusions from a "kidney disease: improving global outcomes" (KDIGO) controversies conference. *Kidney Int.* 2017;91(2):284-293. https://doi.org/10.1016/j.kint.2016.10.004.

8. Arends M, Biegstraaten M, Hughes DA, et al. Retrospective study of long-term outcomes of enzyme replacement therapy in Fabry disease: analysis of prognostic factors. *PLoS One.* 2017;12 (8):e0182379. https://doi.org/10.1371/journal.pone.0182379.

9. Shen JS, Meng XL, Moore DF, et al. Globotriaosylceramide induces oxidative stress and up-regulates cell adhesion molecule expression in Fabry disease endothelial cells. *Mol Genet Metab.* 2008;95(3):163-168. https://doi.org/10.1016/j.ymgme.2008.06.016.

10. Lücke T, Höppner W, Schmidt E, Illsinger S, Das AM. Fabry disease: reduced activities of respiratory chain enzymes with decreased levels of energy-rich phosphates in fibroblasts. *Mol Genet Metab.* 2004;82(1):93-97. https://doi.org/10.1016/j.ymgme.2004.01.011 PMID: 15110329.

11. De Francesco PN, Mucci JM, Ceci R, Fossati CA, Rozenfeld PA. Fabry disease peripheral blood immune cells release inflammatory cytokines: role of globotriaosylceramide. *Mol Genet Metab.* 2013;109(1):93-99, ISSN 1096-7192. https://doi.org/10.1016/j.ymgme.2013.02.003.

12. Weidemann F, Beer M, Kralewski M, Siwy J, Kampmann C. Early detection of organ involvement in Fabry disease by biomarker assessment in conjunction with LGE cardiac MRI: results from the SOPHIA study. *Mol Genet Metab.* 2019;126(2): 169-182. https://doi.org/10.1016/j.ymgme.2018.11.005 PMID: 30594474.

13. Liebau MC, Braun F, Höpker K, et al. Dysregulated autophagy contributes to podocyte damage in Fabry's disease. *PLoS One.* 2013;8(5):e63506.

14. Eikrem Ø, Skrunes R, Tøndel C, et al. Pathomechanisms of renal Fabry disease. *Cell Tissue Res.* 2017;369(1):53-62. https://doi.org/10.1007/s00441-017-2609-9.

15. Fogo AB, Bostad L, Svarstad E, et al. All members of the International Study Group of Fabry Nephropathy (ISGFN). Scoring system for renal pathology in Fabry disease: report of the International Study Group of Fabry Nephropathy (ISGFN). *Nephrol Dial Transplant.* 2010;25(7):2168-2177. https://doi.org/10.1093/ndt/gfp528.

16. Prabakaran T, Birn H, Bibby BM, et al. Long-term enzyme replacement therapy is associated with reduced proteinuria and preserved proximal tubular function in women with Fabry disease. *Nephrol Dial Transplant.* 2014;29(3):619-625. https://doi.org/10.1093/ndt/gft452.

17. Todkar K, Ilamathi HS, Germain M. Mitochondria and lysosomes: discovering bonds. *Front Cell Dev Biol.* 2017;5:106. https://doi.org/10.3389/fcell.2017.00106.

18. Pickles S, Vigié P, Youle RJ. Mitophagy and quality control mechanisms in mitochondrial maintenance. *Curr Biol.* 2018;28 (4):R170-R185. https://doi.org/10.1016/j.cub.2018.01.004.

19. Emma F, Montini G, Parikh SM, Salviati L. Mitochondrial dysfunction in inherited renal disease and acute kidney injury. *Nat Rev Nephrol.* 2016;12(5):267-280. https://doi.org/10.1038/nrneph.2015.214.

20. Jesinkey SR, Funk JA, Stallons LJ, et al. Formoterol restores mitochondrial and renal function after ischemia-reperfusion injury. *J Am Soc Nephrol.* 2014;25(6):1157-1162. https://doi.org/10.1681/ASN.2013090952.

21. Eiyama A, Okamoto K. PINK1/Parkin-mediated mitophagy in mammalian cells. *Curr Opin Cell Biol.* 2015;33:95-101. https://doi.org/10.1016/j.ceb.2015.01.002 PMID: 25697963.

22. Morigi M, Perico L, Benigni A. Sirtuins in renal health and disease. *J Am Soc Nephrol.* 2018;29(7):1799-1809. https://doi.org/10.1681/ASN.2017111218.

23. Bhargava P, Schnellmann RG. Mitochondrial energetics in the kidney. *Nat Rev Nephrol.* 2017;13(10):629-646. https://doi.org/10.1038/nrneph.2017.107.

24. Ruppert T, Schumann A, Gröne HJ, et al. Molecular and biochemical alterations in tubular epithelial cells of patients with isolated methylmalonic aciduria. *Hum Mol Genet.* 2015;24(24): 7049-7059. https://doi.org/10.1093/hmg/ddv405.

25. Litzkas P, Jha KK, Ozer HL. Efficient transfer of cloned DNA into human diploid cells: protoplast fusion in suspension. *Mol Cell Biol.* 1984;4:2549-2552.

26. Small MB, Gluzman Y, Ozer HL. Enhanced transformation of human fibroblasts by origin-deleted simian virus 40. *Nature.* 1982;296:671-672.

27. Shin SH, Park MH, Byeon JJ, et al. A liquid chromatography-quadrupole-time-of-flight mass spectrometric assay for the quantification of Fabry disease biomarker globotriaosylceramide (GB3) in Fabry model mouse. *Pharmaceutics.* 2018;10(2):69. https://doi.org/10.3390/pharmaceutics10020069.

28. Lowry OH, Rosebrough NJ, Farr AL, Randall RJ. Protein measurement with the folin phenol reagent. *J Biol Chem.* 1951;193 (1):265-275.

29. Behringer S, Wingert V, Oria V, et al. Targeted metabolic profiling of methionine cycle metabolites and redox thiol pools in mammalian plasma, cells and urine. *Metabolites.* 2019;9(10): 235. https://doi.org/10.3390/metabo9100235.

30. Whybra C, Kampmann C, Krummenauer F, et al. The Mainz severity score index: a new instrument for quantifying the Anderson-Fabry disease phenotype, and the response of patients to enzyme replacement therapy. *Clin Genet.* 2004;65 (4):299-307. https://doi.org/10.1111/j.1399-0004.2004.00219.x PMID: 15025723.

31. Kang HM, Ahn SH, Choi P, et al. Defective fatty acid oxidation in renal tubular epithelial cells has a key role in kidney fibrosis development. *Nat Med.* 2015;21(1):37-46. https://doi.org/10.1038/nm.3762 PMID: 25419705; PMCID: PMC4444078.

32. Jang HS, Noh MR, Jung EM, et al. Proximal tubule cyclophilin D regulates fatty acid oxidation in cisplatin-induced acute kidney injury. *Kidney Int.* 2020;97(2):327-339. https://doi.org/10.1016/j.kint.2019.08.019 PMID: 31733829; PMCID: PMC6983334.

33. Afshinnia F, Rajendiran TM, Soni T, et al. Michigan Kidney Translational Core CPROBE Investigator Group. Impaired β-oxidation and altered complex lipid fatty acid partitioning

with advancing CKD. *J Am Soc Nephrol*. 2018;29(1):295-306. https://doi.org/10.1681/ASN.2017030350 PMID: 29021384; PMCID: PMC5748913.

34. Jang HS, Noh MR, Kim J, Padanilam BJ. Defective mitochondrial fatty acid oxidation and lipotoxicity in kidney diseases. *Front Med*. 2020;7:65. https://doi.org/10.3389/fmed.2020.00065 PMID: 32226789; PMCID: PMC7080698.

35. Bataille A, Galichon P, Chelghoum N, et al. Increased fatty acid oxidation in differentiated proximal tubular cells surviving a reversible episode of acute kidney injury. *Cell Physiol Biochem*. 2018;47(4):1338-1351. https://doi.org/10.1159/000490819 PMID: 29929186.

36. Singh R, Cuervo AM. Autophagy in the cellular energetic balance. *Cell Metab*. 2011;13(5):495-504. https://doi.org/10.1016/j.cmet.2011.04.004.

37. Najafian B, Fogo AB, Lusco MA, Alpers CE. AJKD atlas of renal pathology: Fabry nephropathy. *Am J Kidney Dis*. 2015;66 (5):e35-e36. https://doi.org/10.1053/j.ajkd.2015.08.006.

38. Maruyama H, Taguchi A, Nishikawa Y, et al. Medullary thick ascending limb impairment in the GlatmTg(CAG-A4GALT) Fabry model mice. *FASEB J*. 2018;32(8):4544-4559. https://doi.org/10.1096/fj.201701374R.

39. Biancini GB, Vanzin CS, Rodrigues DB, et al. Globotriaosylceramide is correlated with oxidative stress and inflammation in Fabry patients treated with enzyme replacement therapy. *Biochim Biophys Acta*. 2012;1822(2):226-232. https://doi.org/10.1016/j.bbadis.2011.11.001.

40. Mookerjee SA, Goncalves RLS, Gerencser AA, Nicholls DG, Brand MD. The contributions of respiration and glycolysis to extracellular acid production. *Biochim Biophys Acta*. 2015;1847 (2):171-181. https://doi.org/10.1016/j.bbabio.2014.10.005.

41. Houten SM, Violante S, Ventura FV, Wanders RJ. The biochemistry and physiology of mitochondrial fatty acid β-oxidation and its genetic disorders. *Annu Rev Physiol*. 2016; 78:23-44. https://doi.org/10.1146/annurev-physiol-021115-105045.

42. Makrecka-Kuka M, Sevostjanovs E, Vilks K, et al. Plasma acylcarnitine concentrations reflect the acylcarnitine profile in cardiac tissues. *Sci Rep*. 2017;7(1):17528. https://doi.org/10.1038/s41598-017-17797-x.

43. Machann W, Breunig F, Weidemann F, et al. Cardiac energy metabolism is disturbed in Fabry disease and improves with enzyme replacement therapy using recombinant human galactosidase A. *Eur J Heart Fail*. 2011;13:278-283.

44. Linkermann A, Skouta R, Himmerkus N, et al. Synchronized renal tubular cell death involves ferroptosis. *Proc Natl Acad Sci U S A*. 2014;111(47):16836-16841. https://doi.org/10.1073/pnas.1415518111. PMID: 25385600; PMCID: PMC4250130.

45. Vatrinet R, Leone G, De Luise M, et al. The α-ketoglutarate dehydrogenase complex in cancer metabolic plasticity. *Cancer Metab*. 2017;5:3. https://doi.org/10.1186/s40170-017-0165-0.

46. Murphy MP, O'Neill LAJ. Krebs cycle reimagined: the emerging roles of succinate and itaconate as signal transducers. *Cell*. 2018;174(4):780-784. https://doi.org/10.1016/j.cell.2018.07.030.

47. Chouchani ET, Pell VR, James AM, et al. A unifying mechanism for mitochondrial superoxide production during ischemia-reperfusion injury. *Cell Metab*. 2016;23:254-263.

48. Rozenfeld P, Feriozzi S. Contribution of inflammatory pathways to Fabry disease pathogenesis. *Mol Genet Metab*. 2017;122 (3):19-27. https://doi.org/10.1016/j.ymgme.2017.09.004.

49. Williams NC, O'Neill LAJ. A role for the Krebs cycle intermediate citrate in metabolic reprogramming in innate immunity and inflammation. *Front Immunol*. 2018;9:141. https://doi.org/10.3389/fimmu.2018.00141.

50. Lampropoulou V, Sergushichev A, Bambouskova M, et al. Itaconate links inhibition of succinate dehydrogenase with macrophage metabolic remodeling and regulation of inflammation. *Cell Metab*. 2016;24:158-166.

51. Shen H, Campanello GC, Flicker D, et al. The human knockout gene CLYBL connects itaconate to vitamin B12. *Cell*. 2017; 171(4):771-782.e11. https://doi.org/10.1016/j.cell.2017.09.051.

52. Tan HWS, Sim AYL, Long YC. Glutamine metabolism regulates autophagy-dependent mTORC1 reactivation during amino acid starvation. *Nat Commun*. 2017;8(1):338. https://doi.org/10.1038/s41467-017-00369-y.

53. Fadel FI, Elshamaa MF, Essam RG, et al. Some amino acids levels: glutamine, glutamate, and homocysteine, in plasma of children with chronic kidney disease. *Int J Biomed Sci*. 2014;10(1):36-42.

54. Wakino S, Hasegawa K, Itoh H. Sirtuin and metabolic kidney disease. *Kidney Int*. 2015;88(4):691-698. https://doi.org/10.1038/ki.2015.157.

55. Farghali H, Kutinová Canová N, Lekić N. Resveratrol and related compounds as antioxidants with an allosteric mechanism of action in epigenetic drug targets. *Physiol Res*. 2013;62 (1):1-13.PMID: 25987173. https://doi.org/10.1016/j.beem.2014.10.003.

56. Luciani A, Schumann A, Berquez M, et al. Impaired mitophagy links mitochondrial disease to epithelial stress in methylmalonyl-CoA mutase deficiency. *Nat Commun*. 2020;11 (1):970. https://doi.org/10.1038/s41467-020-14729-8 Erratum in: Nat Commun. 2020 Apr 1;11(1):1719. PMID: 32080200; PMCID: PMC7033137.

SUPPORTING INFORMATION

Additional supporting information may be found online in the Supporting Information section at the end of this article.